Quantized Output Observer-based Data Driven Model-free Adaptive Control

Bing Ren[1,2] and Guangqing Bao[3*]

[1] *College of Electrical and Information Engineering, Lanzhou University of Technology, Lanzhou, China*
[2] *School of Automation and Electrical Engineering, Lanzhou Jiaotong University, Lanzhou, China*
[3] *School of Electronics & Information Engineering, Southwest Petroleum University, Chengdu, China*
[*] *Corresponding author. E-mail: baogq03@163.com*

Received: Dec. 05, 2022; Accepted: Mar. 13, 2023

This paper studies the quantized output data observer-based data-driven model-free adaptive control(qMFAC) for discrete-time nonlinear systems with unknown structures and network transmission constraints. First, an adaptive observer based on quantized output data is generated with the use of a logarithmic quantizer, and a pseudo-biased derivative(PPD) estimation scheme based on the output quantized data observer is proposed. By dynamic linearization(DL) techniques, a incomplete equivalent data model containing quantized output data are built. Then, the observer output is used to develop a data-driven model-free adaptive control strategy that only makes use of quantified output and input. With the Lyapunov function and sector boundary approaches, the bounded tracking performance of the proposed qMFAC is strictly theoretical analyzed, and the effectiveness of qMFAC is verified through numerical simulation and simulation experiments of the shell and tube heat exchanger control system.

Keywords: Quantized output data; Adaptive observer; Data-driven; Logarithmic quantizer; Pseudo-partial derivative;

http://dx.doi.org/10.6180/jase.202402_27(2).0004

1. Introduction

The Network control system has been paid more and more attention to because of its high reliability, low maintenance cost, flexible configuration, and simple installation [1–4]. The conflict between difficult control tasks and scarce network resources has, however, progressively emerged as a result of the coupling of control systems and network systems [5–7]. Quantization according to specific rules before transmission is a good choice since it can reduce the signal transmission frequency of the network control system and take up less network resources. The processed data is called incomplete data, which is usually a finite or infinite set of discrete data [8–10].

According to the different types of data, scholars have studied the control systems containing quantized output data [11–13], quantized input data [14–16], quantized error information [17–19]. For instance, the literature [12]focuses on the novel dissipative sampled-data control mechanism for high-speed train systems with quantized measurements. To prevent the impact of quantization error on the tracking performance, [13] takes into account the uniform quantizer with an encoding and decoding technique in place of the logarithmic quantizer. Chu and Li [14] addresses the problem of robust integrated fault estimation and fault-tolerant control for a class of discrete-time networked Takagi-Sugeno fuzzy systems with two-channel event-triggered schemes and input quantization. Ha et al. [15] and Qiu et al. [16]investigates the neural network and fuzzy backstepping control separately for fractional-order nonlinear systems with quantized input. Zero error tracking is made possible by comparing the output with the provided reference and locally quantizing the error rather than directly quantizing output, as inspired by [11]. After

that, it is sent back to the controller for further update in [17]. Then, [18] extended this to linear and affine nonlinear stochastic systems. The quantization process of the above research is founded on a precise system model or structure. For nonlinear control systems with unknown structure, model, or parameter uncertainty, however, research on replacing the original data with quantitative data is somewhat constrained.

Data-driven control uses the input and output data of the system to replace the complicated mathematical modeling link that requires clear structural parameters and realizes the control of complex systems [20] . As one of the typical data-driven controls, model-free adaptive control (MFAC) has gained popularity due to its distinctive online data DL method and the introduction of the novel PPD idea [21]. It has been applied in electric power [22–24],industrial [25, 26], transportation [27, 28] and other systems. However, the data in the above controllers is complete. In other words, all the data output by the system is used to estimate PPD, create dynamic data model and generate control signal. With the development of networked control systems, it has become more difficult to increase data transmission efficiency while maintaining system stability. By decoding the output and tracking error through the use of logarithmic quantizer, [23] established MFAC with quantized output information and then proved that the tracking error of the system is bounded. To suppress the influence of data quantization, an improved MFAC algorithm can achieve the goal of zero-tracking error is proposed in [29]. In [30], the problem of quantized distributed bipartite consensus tracking control is addressed for unknown nonlinear discrete-time multi-agent systems. However, the above research uses the parameter estimation criterion function to estimate PPD and design controller. The output and the increments of two adjacent operating points are the key components in the criterion function and must be quantized. This not only raises the operating cost of the actual industrial site, but also increases the steady-state error due to the introduction of too many quantization errors, making the control effect unsatisfactory, which is the motivation for the research in this paper.

Inspired by the above discussion, this paper designs an observer which takes the quantized output data as input and compensates the quantization error by the gain of the observer, thus improving the control accuracy. Morever, a new observer-based PPD estimation algorithm and an incomplete data-driven model-free adaptive control scheme, which depends only on the input and quantized output data, are developed. Compared with [23], it avoids the superposition of quantization error caused by quantized output data and quantized output incremental data acting directly on the control system, reduces the steady-state error, and enhances the transmission effect, which is more beneficial to the controller design.

2. Problem formulation

Consider the discrete-time SISO nonlinear systems as follows:

$$\begin{aligned} y(k+1) = f(&y(k), y(k-1), \cdots \\ &y\left(k-t_y\right), u(k), u(k-1), \cdots, u\left(k-t_u\right)) \end{aligned} \tag{1}$$

Where k represents the sampling work point, $y(k)$ and $u(k)$ are the system output, and input at the kth working point, respectively, $f(\cdot)$ is a nonlinear function with unknown structure and parameters, the integers t_y and t_u represent the order of system output and input separately.

2.1. Equivalent dynamic linearized data model

For the systems (1), the following two assumptions should be given first.

Assumption 1. The unknown nonlinear function $f(\cdot)$ is derivable and continuous at any time concerning control input $u(k)$.

Assumption 2. The nonlinear systems (1) satisfy Lipschitz condition. Namely, there is a constant μ, so that $\Delta y(k+1) \leq \mu \Delta u(k)$. where $\Delta y(k+1) = y(k+1) - y(k)$ indicates output increments, $\Delta u(k) = u(k) - u(k-1)$ means input increment. the input rate of change between two adjacent work point $\Delta u(k)$ is uniformly bounded, that is, $|\Delta u(k) \leq \zeta|$.

Remark 1. Assumption 1 is general for controller design. Assumption 2 can be said to be an embodiment of the law of conservation of energy. The amount of control input and input increment determine the amount of output and output increment. If the input change rate of $\Delta u(k)$ for two consecutive work points is too large, the stability of system will quickly deteriorate. This assumption will also make the theoretical analysis more suitable for practical applications, such as the three-tank [21] and automatic parking control systems [27].

According to the DL method, when $\Delta u(k) \neq 0$, the system(1) can be represented as an equivalent model based on input and output data:

$$y(k+1) = y(k) + \psi(k)\Delta u(k) \tag{2}$$

Where $\psi(k)$ represents the PPD. $\psi(k)$ is bounded because of Assumption 2 , that is $|\psi(k)| \leq \mu$.

Remark 2. $\psi(k)$ is one of the characteristics of the DL method. Numerically, it is slowly time-varying data. From

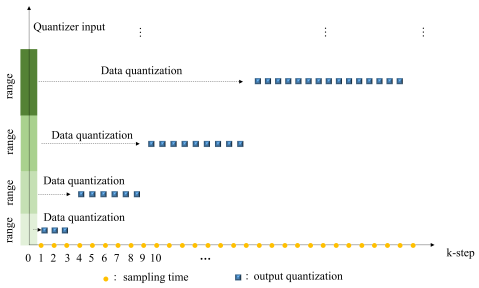

Fig. 1. Conceptual framework of the output data quantification strategy.

the perspective of data meaning, it is also highly complex, which may include such time-varying structure, parameters, or order information. From the point of view of physical meaning, it does not exist, which some scholars describe as non-parametric.

Remark 3. Because only I/O data and $\psi(k)$ are needed, the equivalent data model (2) is particularly suitable for the analysis of nonlinear systems with unknown nonlinear systems. To obtain the mysterious $\psi(k)$, we cannot be obtained it directly. It is necessary to use estimation algorithms, such as an improved projection algorithm or a least squares algorithm with a time-varying forgetting factor.

2.2. Data quantification

For control systems with constrained network resources, data quantization is one of the most efficient ways to conserve resources. When a quantizer is positioned in between a sensor and a controller, it quantizes the output data and uses it to produce control signals. The control signal is quantized and applied to the controlled item if the sensor is swapped out for an actuator. This article focuses on the design of controllers using quantized output data.

The logarithmic quantizer is selected, and the quantized data set is given by:

$$\begin{aligned}\Xi = &\left\{\pm\kappa^{\sigma} : \kappa^{\sigma} = {v_y}^{\sigma}\kappa^{0}, \sigma = \pm1, \pm2, \cdots\right\} \\ &\cup \left\{\kappa^{0}\right\} \cup \{0\}, 0 < v_y < 1, \kappa^{0} > 0\end{aligned} \tag{3}$$

Where v denotes quantifier density, $\kappa^0 > 0$ is quantified initial value.

The output quantizer is given by:

$$q(y(k)) = \begin{cases} \kappa^{\sigma} & \text{if } \frac{\kappa^{\sigma}}{1+\gamma_y} < y(k) \leq \frac{\kappa^{\sigma}}{1-\gamma_y} \\ 0 & \text{if } y(k) = 0, \\ -q(-y(k)) & \text{if } y(k) < 0. \end{cases} \tag{4}$$

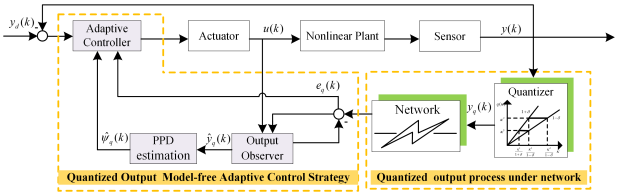

Fig. 2. Structure of the quantized output observer-based model-free adaptive control scheme.

where $q(y(k))$ is the quantized output When the input of the quantizer is $y(k)$, γ_y denotes output quantizer parameters, $\gamma_y = \frac{1-v_y}{1+v_y}$, namely $0 < \gamma_y < 1$.

The conceptual framework of the data output quantization process is shown in Fig. 1. The sampling interval is shown by the horizontal axis, and the quantization input range, which is divided into various color segments, is represented by the vertical axis. The identical quantization level will be produced for all inputs with the same color range. The quantization density of the quantizer determines the size of the quantization range. Correspondingly, larger densities result in smaller ranges, higher quantization accuracy, and lower transmission efficiencies. All output data are used to create control signals when the density is equal to 1.

In this paper, our control objective is to design a data-driven model-free adaptive controller using quantized output data to achieve trajectory tracking control. The block diagram is shown in Fig.2.The left dashed box in Fig.2 shows the model-free adaptive control strategy containing the quantized output observer, PPD estimation and controller, while the right dashed box shows the quantization process of the output data.

3. Quantized output data observer based model-free adaptive control design

3.1. PPD estimation

An adaptive observer is introduced between the quantizer and the controller, and its structure is as follows:

$$\hat{y}_q(k+1) = \hat{y}_q(k) + \hat{\psi}(k)\Delta u(k) + k_q e_q(k) \tag{5}$$

Where $\hat{y}_q(k)$ and $\hat{\psi}(k)$ are the estimated value of the quantized output and PPD at work point of k, the gain k_q is chosen such that $0 < k_q < 1, e_q(k)$ is the quantized output estimation error, denoted as:

$$e_q(k) = y_q(k) - \hat{y}_q(k) \tag{6}$$

Where $y_q(k)$ is the output of the quantizer, that is $y_q(k) = q(y(k))$. From Eqs. (5) and (6), we can obtain:

$$y_q(k+1) = \hat{y}_q(k) + \hat{\psi}(k)\Delta u(k) + k_q e_q(k) + e_q(k+1) \tag{7}$$

Using sector bound method, y(k) and $y_q(k)$ satisfies the following relationships:

$$y_q(k) - y(k) = \beta_y y(k) \tag{8}$$

Where $|\beta_y| < \gamma_y$, that means $0 < \beta_y < 1$.

In this way, combining Eqs. (2), (5), (6) and (8), the dynamic characteristics of the observation error can be deduced:

$$e_q(k+1) = M_q e_q(k) + \tilde{\psi}(k)\Delta u(k) + \beta_y \psi(k)\Delta u(k) \tag{9}$$

where $\tilde{\psi}(k) = \psi(k) - \psi(\hat{k})$, denotes the PPD parameter estimation error. $M_q = 1 - k_q$, satisfying $0 < M_q < 1$.

The PPD estimation algorithm is built based on the structure of the quantized output data observer Eq. (5):

$$\hat{\psi}(k+1) = \hat{\psi}(k) + \Delta u(k)\Theta_q(k)\left(e_q(k+1) - M_q e_q(k) - \beta_y \psi(k)\Delta u(k)\right) \tag{10}$$

Where $\Theta_q(k) = 2/\left(|\Delta u^2(k)| + \eta\right)$, let $\epsilon = \zeta^2 + \eta, \Theta_q(k) \geq 2/\left(\zeta^2 + \eta\right)$ by Assumption 2.

Remark 4. To ensure that the PPD estimation algorithm has a more vital tracking ability for timevarying parameters, set a small positeve constant ρ as reset threshold value, the retune mechanism will work when $|\hat{\psi}(k)| \leq \varrho$ or $|\Delta u(k-1)| \leq \varrho$, that is, $\hat{\psi}(k) = \hat{\psi}(1)$, where $\hat{\psi}(1)$ is the initial value.

3.2. Controller design and stability analysis

Based on the PPD estimation algorithm(10), in order to realize the nonlinear control system (1) to track the given trajectory well, the following controllers are designed:

$$u(k) = u(k-1) + \frac{\hat{\psi}(k)\left(y_d(k+1) - \hat{y}_q(k) - k_q e_q(k)\right)}{\hat{\psi}^2(k) + \omega} \tag{11}$$

Where $y_d(k)$ is the bounded expected trajectory, that is $|y_d(k)| \leq Y_M, \omega > 0$ is a weighting factor.

Theorem 1. For the nonlinear system Eq. (1) satisfying Assumptions 1-2, quantized by mechanism Eqs. (3) and (4), control laws Eqs. (9) and (10) ensure the tracking error convergence to a bounded region by $\lim_{k\to\infty} e(k) \leq \left(\frac{2a_1}{1-a_0} + \frac{\beta_y}{1+\beta_y}\right) Y_M$, where $a_0 = \frac{\omega}{\hat{\psi}^2(k)+\omega}$, $a_1 = \frac{\omega}{(1+\beta_y)\left(\hat{\psi}^2(k)+\omega\right)}$

Proof. The system tracking error is defined as follows:

$$e(k) = y_d(k) - y(k) \tag{12}$$

Both the process of output data passing through the quantizer and output quantized data crossing the observer generate corresponding errors, and they all have some relationship with the tracking error. Therefore, it is necessary to discuss the boundedness of $e_q(k)$, $\hat{\psi}(k)$, observer tracking error, and quantizer tracking error to derive the convergence performance of the system tracking error.

1. Boundedness of $e_q(k)$ and $\hat{\psi}(k)$

   Subtracting $\psi(k+1)$ on both sides of (10) yields:

$$\tilde{\psi}(k+1) = \left(1 - \Delta u^2(k)\Theta_q(k)\right)\tilde{\psi}(k) \tag{13}$$

Consider the Lyapunov function as below:

$$V(k) = \rho e_q^2(k) + \chi \tilde{\psi}^2(k) \tag{14}$$

Substitute Eq. (9) and Eq. (13) into Eq. (14), then we can obtain:

$$\Delta V(k+1) = V(k+1) - V(k) \tag{15}$$

$$\begin{aligned}\Delta V(k+1) &= V(k+1) - V(k)\\ &= \rho\left(M_q^2 - 1\right)e_q^2(k) + \rho\left(\tilde{\psi}^2(k)\Delta u^2(k)\right.\\ &+ \beta_q^2\psi^2(k)\Delta u^2(k) + 2M_q e_q(k)\tilde{\psi}(k)\\ &\times \Delta u(k) + 2\beta_y\tilde{\psi}(k)\Delta u(k)\psi(k)\Delta u(k)\\ &\left.+2\beta_y M_q e_q(k)\psi(k)\Delta u(k)\right) - \chi\\ &\times\left(\eta\Theta_q^2(k)\right)\tilde{\psi}^2(k)\Delta u^2(k)\end{aligned} \tag{16}$$

According to the principle of basic inequality, Eq. (15) is simplified as:

$$\begin{aligned}\Delta V(k+1) &\leq \left(\rho M_q^2 - \rho + \rho^2\varsigma_1 + \frac{\rho\beta_y^2}{\varsigma_2}\right)e_q^2(k)\\ &+ \left(\rho^2\zeta_3\beta_y^2 + \rho + \frac{M_q^2}{\varsigma_1} - \chi\eta\epsilon^2\right)\\ &\times \tilde{\psi}^2(k)\Delta u^2(k)\\ &+ \left(\frac{1}{\zeta_3} + \rho\beta_y^2 + \rho^2\varsigma_2 M_q^2\right)\psi^2(k)\Delta u^2(k)\\ &= l_1 e_q^2(k) + l_2\Omega_1^2 + l_3\Omega_2^2\end{aligned} \tag{17}$$

where $\Omega_1 = \tilde{\psi}(k)\Delta u(k), \Omega_2 = \psi(k)\Delta u(k)$. If select appropriate parameters $\varsigma_1, \varsigma_2, \varsigma_3, \rho$ and χ, satisfy the following inequalities:

$$\begin{cases} l_1 = \rho M_q^2 - \rho + \rho^2 \varsigma_1 + \frac{\rho \beta_y^2}{\varsigma_2} < 0 \\ l_2 = \rho^2 \varsigma_3 \beta_y^2 + \rho + \frac{M_q^2}{\varsigma_1} - \chi \eta \epsilon^2 < 0 \\ l_3 = \frac{1}{\varsigma_3} + + \rho \beta_y^2 + \rho^2 \varsigma_2 M_q^2 < 0 \end{cases} \tag{18}$$

then, $\Delta V(k+1) \leq 0$, indicates that $V(k)$ decreasing gradually. Because of $V(k) > 0$, it converges to a constant $V(\infty)$, that is $\Delta V(k) \to 0$. Therefore $\lim_{k\to\infty} e_q(k) = 0, \tilde{\psi}(k)$ is bounded, cause $\hat{\phi}$ is bounded also.

2. Boundedness of observer tracking error

Consider observer tracking error as $\hat{e}_q(k) = y_d(k) - \hat{y}_q(k)$, substitute Eq. (5) and Eq. (11) yields:

$$\begin{aligned} \hat{e}_q(k+1) &= y_d(k+1) - \hat{y}_q(k+1) \\ &= y_d(k+1) - \hat{y}_q(k) \\ &- \frac{\hat{\psi}^2(k)}{\hat{\psi}^2(k)+\omega} \left(y_d(k+1) - \hat{y}_q(k) \right. \\ &\left. - \hat{y}_q(k) - k_q e_q(k) \right) - k_q e_q(k) \\ &= \frac{\omega}{\hat{\psi}^2(k)+\omega} \left(\hat{e}_q(k) + \Delta y_d(k+1) - k_q e_q(k) \right) \end{aligned} \tag{19}$$

Since $0 < \omega < \hat{\psi}^2(k) + \omega$, there is $0 < \frac{\omega}{\hat{\psi}^2(k)+\omega} = a_0 < 1$, by the absolute value inequality, we have:

$$\begin{aligned} \left|\hat{e}_q(k+1)\right| &\leq a_0 \left|\hat{e}_q(k)\right| + a_0 \left|k_q\right| \left|e_q(k)\right| + a_0 \left|\Delta y_d(k+1)\right| \\ &\leq a_0^2 \left|\hat{e}_q(k-1)\right| + a_0^2 \left|k_q\right| \left|e_q(k-1)\right| \\ &+ 2a_0^2 Y_M + a_0 \left|k_q\right| \left|e_q(k)\right| + 2a_0 Y_M \leq \cdots \\ &\leq a_0^k \left|\hat{e}_q(1)\right| \\ &+ \frac{\left(a_0 \left|k_q\right| \left|e_q(k)\right| + 2a_0 Y_M\right) \left(1 - a_0^k\right)}{1 - a_0} \end{aligned} \tag{20}$$

Where $\lim_{k\to\infty} a_0^k \to 0$, it follows that $\hat{e}_q(k)$ is bounded, bring in $\lim_{k\to\infty} e_q(k) = 0$ to (23), thus there is $\lim_{k\to\infty} \hat{e}_q(k) \leq \frac{2a_0\gamma_M}{1-a_0}$.

3. Boundedness of quantifier tracking errors

Quantifier tracking error is defined as:

$$\tilde{e}_q(k) = y_d(k) - y_q(k) \tag{21}$$

where $\tilde{e}_q(k), e_q(k)$ and $\hat{e}_q(k)$ satisfy a particular relationship: $\tilde{e}_q(k) = \hat{e}_q(k) - e_q(k)$, both $e_q(k)$ and $\hat{e}_q(k)$ in the equation are proven. The quantifier tracking error is also bounded, satisfying

$$\lim_{k\to\infty} \tilde{e}_q(k) \leq \frac{2a_0\gamma_M}{1-a_0}$$

4. Boundedness of tracking errors

Considering the above error in relation to the tracking error, take Eqs. (7) and (8) to Eq. (11):

$$\begin{aligned} e(k+1) &= y_d(k+1) - \frac{1}{1+\beta_y} y_q(k+1) \\ &= \frac{1}{1+\beta_y} \left(\frac{\omega}{\hat{\psi}^2(k)+\omega} \left(y_d(k+1) - \hat{y}_q(k) - k_q e_q(k) \right) \right. \\ &\left. - e_q(k+1) + \beta_y y_d(k+1) \right) \\ &= a_1 \left(\tilde{e}_q(k) + \left(1 - k_q\right) e_q(k) + \Delta y_d(k+1) \right) \\ &- \frac{e_q(k+1)}{1+\beta_y} + \frac{\beta_y y_d(k+1)}{1+\beta_y} \end{aligned} \tag{22}$$

Where $a_1 = \frac{\omega}{\left(1+\beta_y\right)\left(\hat{\psi}^2(k)+\omega\right)}$, since $1 + \beta_y > 1$, it can be deduced that $\omega < \hat{\psi}^2(k) + \omega < \left(1 + \beta_y\right)\left(\hat{\psi}^2(k) + \omega\right)$, so $0 < a_1 < 1$. Taking absolute values on both sides:

$$\begin{aligned} \left|e(k+1)\right| &\leq a_1 \left|\tilde{e}_q(k)\right| + a_1 \left(1 - k_q\right) \left|e_q(k)\right| \\ &+ 2a_1 Y_M + \frac{\left|e_q(k+1)\right|}{1+\beta_y} + \frac{\beta_y Y_M}{1+\beta_y} \end{aligned} \tag{23}$$

Where the convergence of $e_q(k)$ and $\tilde{e}_q(k)$ has been derived previously. Carrying them into the above equation(30) gives $\lim_{k\to\infty} e(k) \leq \left(\frac{2a_1}{1-a_0} + \frac{\beta_y}{1+\beta_y} \right) Y_M$. If the given trajectory $y_d(k)$ is a constant, that is $\Delta y_d(k+1) = 0$, then $\lim_{k\to\infty} e(k) \leq \frac{\beta_y}{1+\beta_y} Y_M$

Remark 5. The scheme in [23] requires the quantization output and increment output to design the PPD and controller, which will produce two different quantization errors, making the control more difficult. In this paper, we only need to quantify the output data, and minimize the impact of quantization error on the system by constructing the observer and reasonably selecting the observer gain.

4. Simulation

In this section, we verify the effectiveness of the proposed algorithm through two simulation experiments. The first is a numerical simulation, and the second is a simulation of a model of a shell and tube heat exchanger commonly used in industry. Despite the mathematical models for both examples are shown, they are only employed to provide input and output data and have no bearing on how the controller was designed.

The QMFAC [23] scheme as follows is used for comparison.

$$\begin{aligned}\hat{\phi}(k) &= \hat{\phi}(k-1) + \frac{\eta \Delta u(k-1)}{\mu + |\Delta u(k-1)|^2}\left(q_\Delta(\Delta y(k))\right. \\ &\left. - \hat{\phi}(k-1)\Delta u(k-1)\right) \\ u(k) &= u(k-1) + \frac{\rho \hat{\phi}(k)}{\lambda + |\hat{\phi}(k)|^2}\left(y^*(k) - q_y(y(k))\right)\end{aligned} \tag{24}$$

Where $q_y(y(k))$ and $q_\Delta(\Delta y(k))$ represent the quantization of output increment and output data respectively. The values of the parameters in the scheme will be given in the following simulation experiments.

4.1. Example 1

The SISO nonlinear system is selected as follows:

$$y(k+1) = \sin(y(k)) + u(k)(3 - \sin(y(k))u(k)) \tag{25}$$

Set the desired tracking trajectory expressed as:

$$\begin{aligned}y_d(k+1) &= 0.2 + 0.3(\sin((2k\pi/200) \\ &+ \sin((2k\pi/100)) + \sin((2k\pi/50)))\end{aligned} \tag{26}$$

The working point is set to $[0, 1000]$. The parameters of proposed controller are $k_q = 0.8, \omega = 0.01, \eta = 2.7, \hat{\psi}(1) = 21, \varrho = 0.0001, \kappa^0 = 10, \sigma = (1, 2, \cdots, 500), v_y = 0.9$. Parameters of *QMFAC* are selected as $\rho = 1, \eta = 1, \lambda = 2, \mu = 1, \theta_\Delta = \theta_y = 0.9$ and $z_0 = 5$. The simulation output performance results are depicted in Fig.3. It can be seen that the proposed qMFAC method can achieve a better performance in the presence of quantitative output data. In comparison, the output of QMFAC exhibits a larger tracking error because of the simultaneous presence of the output quantizer and the output incremental quantizer, the quantization error increases exponentially and finally acts on the dynamic performance, the PPD estimate of qMFAC changes more slowly than that of QMFAC.

Remark 6. When given trajectory $y_d(k)$ is a constant, the tracking error of the *QMFAC* is $\lim_{k\to\infty} e(k) \leq \frac{\delta_y Y_M}{d_1}$ with denominator $d_1 < 1$, while in this paper $\lim_{k\to\infty} e(k) \leq \frac{\beta_y}{1+\beta_y} Y_M$ with denominator $1 + \beta_y > 1$. Both using sector-bound method to discuss quantization error, and it is clear that the numerator of the latter is smaller than the former, i.e., $\beta_y < \delta_y$. Therefore, theoretically, the proposed in this paper outperforms QMFAC in terms of tracking effect, and it is verified in Fig.3.

The quantization outputs of qMFAC and QMFAC are shown in Fig.4. The horizontal and vertical coordinates indicate the number of quantization levels and the number of transmissions, respectively. It can be seen that the number of orange quantization levels representing the proposed qMFAC is less than that of blue ones representing the comparison scheme, and the tracking effect is better with fewer quantization levels.

Different control will make different quantization levels at the same quantization density, and different quantization densities will also affect the quantization levels. Four quantizers with quantization densities of 0.95, 0.9, 0.85, and 0.8 were selected from high to low and used in the above experiments to verify this claim. The tracking error of the system obtained is shown in Fig.5. As the quantization density decreases, the quantization level becomes coarser, the gap between the real output value and the actual output value increases, and the tracking error increases accordingly. However, the proposed scheme is not repeatedly used a quantizer, the quantization error is introduced less, and its overall tracking error is always smaller than QMFAC. Table1 lists the quantization levels produced by the proposed and scheme[23] for each of the four densities. As the quantization density decreases, the quantization level becomes coarser and the difference between different methods becomes smaller. When the quantization density is 0.95 , the proposed method has a better convergence effect than QMFAC while saving 21.2% of transmission channel resources.

4.2. Example 2

In industrial production, specialized heat exchangers are required to prevent the direct mixing of hot and cold fluids. Shell and tube heat exchangers are the most widely used wall-to-wall heat exchange devices. However, it have an assertive uncertain nonlinear behavior limited by operating conditions and material characteristics.

As shown in Fig. 6, the cold fluid enters from the liquid inlet, flows through the inside of the tube bundle and finally exits from the liquid outlet when the shell and tube heat exchanger is in operation. The hot fluid flows in from the steam inlet, around the gap between the heat exchanger tube plate and the tube bundle, and out through the steam outlet. The hot and cold fluids are separated by multiple thin tube walls of the tube bundle. The hot fluid first transfers heat to the thin tube walls, and then the tube walls transfer heat to the cold fluid inside the tube, completing the entire heat transfer process.

Keeping the steam flow constant, this paper consider process water flow rate as input and process water exit temperature as output, the Hammerstein model of Eq. (24) is used to describe the dynamic behavior of the heat exchanger as:

$$\begin{aligned}G_H\left(z^{-1}\right) &= \frac{1.2z^{-1} - 0.1z^{-2}}{1 - 0.6z^{-1} + 0.1z^{-2}} \\ N(u) &= 1.5u(k) - 1.5u^2(k) + 0.5u^3(k)\end{aligned} \tag{27}$$

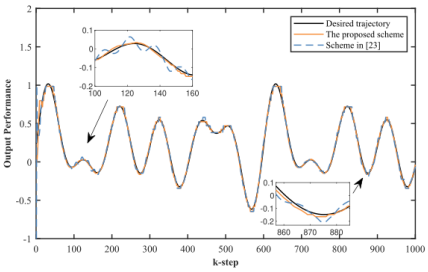

(a) Output performance of the system.

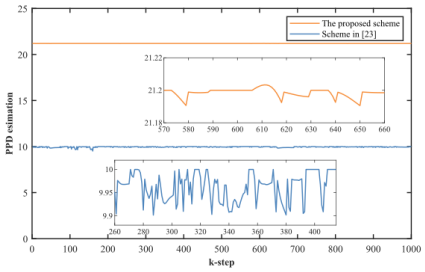

(b) PPD estimation.

Fig. 3. Tracking performance of the system.

Table 1. Quantization levels at different densities.

	$v_y = 0.95$	$v_y = 0.9$	$v_y = 0.85$	$v_y = 0.8$
Proposed scheme	155	94	67	52
Scheme [23]	198	108	79	57
Level savings	21.72%	12.96%	15.19%	8.77%

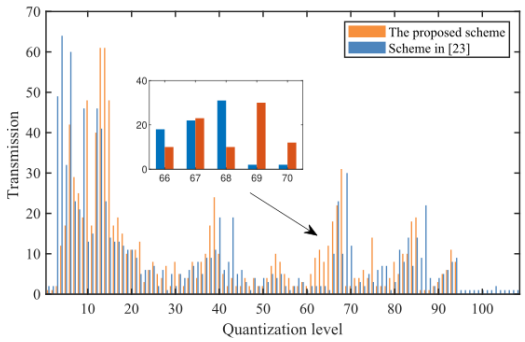

Fig. 4. Quantizaion leves and transmission.

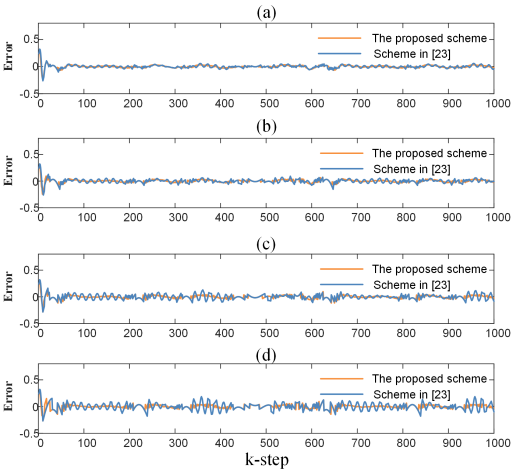

Fig. 5. Error performance at four different densities:(a) $v_y = 0.95$. (b) $v_y = 0.9$. (c) $v_y = 0.85$. (d) $v_y = 0.8$.

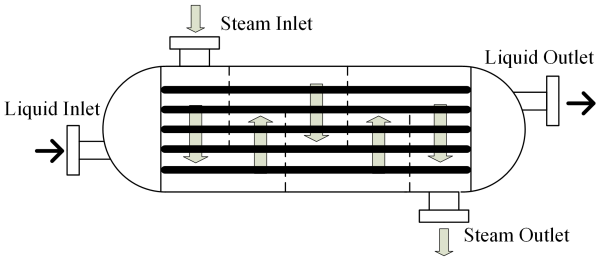

Fig. 6. Shell and tube heat exchanger.

The following reference signals have been selected to match the temperature requirements of industrial pipeline fluids closely:

$$y_d(k) = \begin{cases} 30 & \text{if } k \leq 500 \\ 60 & \text{if } 500 < k \leq 1000 \end{cases} \tag{28}$$

The proposed controller parameters are set as $k_q = 0.8, \hat{\psi}(1) = 80, \kappa^0 = 83, v_y = 0.9$, and the rest of the parameters remain unchanged. Parameters of *QMFAC* are selected as $\rho = 1, \eta = 1, \lambda = 2, \mu = 1, \theta_\Delta = \theta_y = 0.9$ and $z_0 = 5$. The system output performance of the heat exchanger with quantized output data is shown in Fig. 7. When $y_d(k) = \text{const}$, both can track the given temperature quickly, and the proposed control method has a small overshoot, fast convergence, and high accuracy.

The tracking error and control input performance are given in Fig. 8. It can be seen that the proposed method converges to a relatively small neighborhood from the equilibrium point with good steady-state performance for both tracking errors and control inputs. Similarly, the tracking effect can be improved by increasing the density. How-

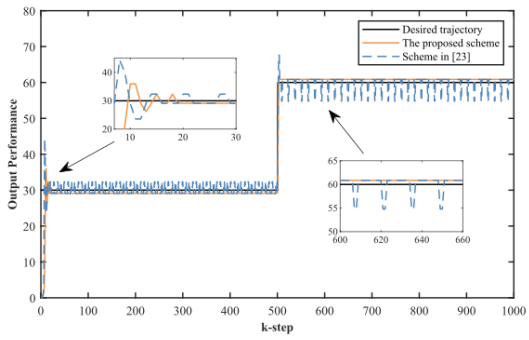

Fig. 7. Output performance of shell and tube heat exchanger.

ever, a certain amount of transmission resources must be sacrificed simultaneously, so a compromise between transmission frequency and control accuracy is needed.

Further, when environmental conditions are added to the simulation experiment, that is the measurement noise 0.5rand(1) and the step disturbance 1 at 200s and another step disturbance -1 at 700s in input channel. The parameters of qMFAC and QMFAC are the same as above, the simulation experimental results as shown in Fig.9. It can be seen that when external interference and noise appear in the environment, the proposed method can respond quickly, and is superior to QMFAC in output tracking performance, error performance and input performance. At the same time, the PPD of QMFAC changes on a slope with a large rate of change, while the PPD based on the quantized output observer only changes slowly after a small amplitude at 200s, 500s and 700s, which is consistent with the characteristics of slow time-varying, it has good control accuracy and quality.

5. Conclusions

This paper presents a data-driven model-free adaptive control strategy for discrete-time nonlinear systems based on quantized output data observer. The output data quantified by the quantifier is used to design model-free adaptive control scheme including the PPD estimation algorithm based on quantized output observer. This change in data type extends the application of MFAC based on the observer framework. Data driven by quantized output is implemented over a limited number of transmission channels, saving valuable network resources. Through the Lyapunov function, the asymptotic stability of the proposed qMFAC algorithm is analyzed, which shows that the system tracking error can achieve final bounded convergence. Finally, a numerical simulation and a shell and tube heat exchanger control system simulation have been made to verify the effectiveness of the proposed algorithm. Compared with the current results, qMAFC designed in this paper is simple, effective, and low-cost, suitable for scaling up to practical applications. In the future, we focus on zero error data driven control with time-varying network induced delay and quantized data.

Acknowledgment

This work was funded by National Natural Science Foundation of China (51967012), Key Research and Development Program of Gansu Province (20YF8GA055), Natural Science Foundation of Gansu Province (22JR5RA359) and Youth Science Foundation of Lanzhou Jiaotong University (2019034).

References

[1] X. Chu and M. Li, (2018) *"Event-triggered fault estimation and sliding mode fault-tolerant control for a class of nonlinear networked control systems"* **Journal of the Franklin Institute** ***355***(13): 5475–5502.

[2] C. Peng, J. Zhang, and Q.-L. Han, (2018) *"Consensus of multiagent systems with nonlinear dynamics using an integrated sampled-data-based event-triggered communication scheme"* **IEEE Transactions on Systems, Man, and Cybernetics: Systems** ***49***(3): 589–599.

[3] H. Liang, L. Chen, Y. Pan, and H.-K. Lam, (2022) *"Fuzzy-based robust precision consensus tracking for uncertain networked systems with cooperative-antagonistic interactions"* **IEEE Transactions on Fuzzy Systems**:

[4] Z. Cao, B. Niu, G. Zong, and N. Xu, (2023) *"Small-gain technique-based adaptive output constrained control design of switched networked nonlinear systems via event-triggered communications"* **Nonlinear Analysis: Hybrid Systems** ***47***: 101299.

[5] X. Liu, J. Zhang, and Y. Xia, (2019) *"Co-design of quantization and event-driven control for networked control systems"* **IEEE Transactions on Systems, Man, and Cybernetics: Systems** ***51***(5): 3103–3110.

[6] L. Cao, Y. Pan, H. Liang, and T. Huang, (2022) *"Observer-Based Dynamic Event-Triggered Control for Multiagent Systems With Time-Varying Delay"* **IEEE Transactions on Cybernetics**:

[7] F. Cheng, H. Wang, L. Zhang, A. Ahmad, and N. Xu, (2022) *"Decentralized adaptive neural two-bit-triggered control for nonstrict-feedback nonlinear systems with actuator failures"* **Neurocomputing** ***500***: 856–867.

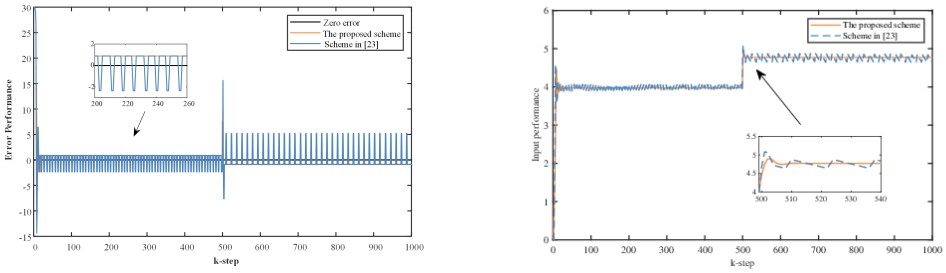

(a) Error performance. (b) Input performance.

Fig. 8. Tracking performance of shell and tube heat exchanger.

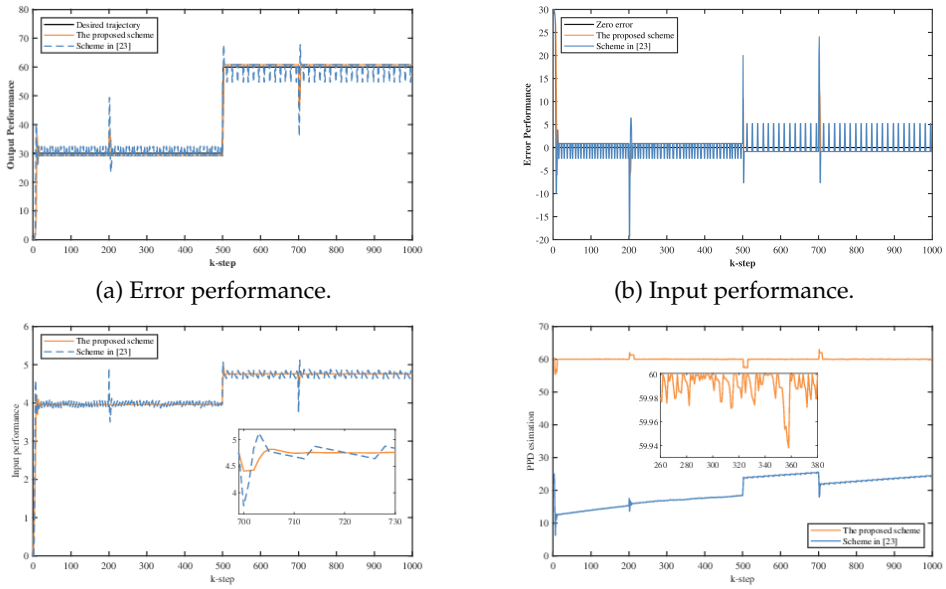

(a) Error performance. (b) Input performance.

(c) Input performance with disturbance. (d) PPD estimation.

Fig. 9. Tracking performance of shell and tube heat exchanger with disturbance.

[8] L. Xing, C. Wen, H. Su, J. Cai, and L. Wang, (2015) *"A new adaptive control scheme for uncertain nonlinear systems with quantized input signal"* **Journal of the Franklin Institute** ***352***(12): 5599–5610.

[9] S. Song, J. H. Park, B. Zhang, and X. Song, (2021) *"Composite adaptive fuzzy finite-time quantized control for full state-constrained nonlinear systems and its application"* **IEEE Transactions on Systems, Man, and Cybernetics: Systems** ***52***(4): 2479–2490.

[10] X. Song, M. Wang, C. K. Ahn, and S. Song, (2021) *"Finite-time fuzzy bounded control for semilinear PDE systems with quantized measurements and markov jump actuator failures"* **IEEE Transactions on Cybernetics** ***52***(7): 5732–5743.

[11] B. Xuhui, W. Taihua, H. Zhongsheng, and C. Ronghu, (2015) *"Iterative learning control for discrete-time systems with quantised measurements"* **IET Control Theory & Applications** ***9***(9): 1455–1460.

[12] X. Cai, K. Shi, S. Zhong, and X. Pang, (2021) *"Dissipative sampled-data control for high-speed train systems with quantized measurements"* **IEEE Transactions on Intelligent Transportation Systems** ***23***(6): 5314–5325.

[13] D. Shen and C. Zhang, (2020) *"Zero-error tracking control under unified quantized iterative learning framework via encoding–decoding method"* **IEEE Transactions on Cybernetics** ***52***(4): 1979–1991.

[14] X. Chu and M. Li, (2019) *"Integrated event-triggered fault estimation and fault-tolerant control for discrete-time fuzzy systems with input quantization and incomplete measurements"* **Journal of the Franklin Institute** ***356***(13): 7112–7143.

[15] S. Ha, L. Chen, H. Liu, and S. Zhang, (2022) *"Command filtered adaptive fuzzy control of fractional-order nonlinear systems"* **European Journal of Control *63***: 48–60.

[16] H. Qiu, H. Liu, and X. Zhang, (2022) *"Composite adaptive fuzzy backstepping control of uncertain fractional-order nonlinear systems with quantized input"* **International Journal of Machine Learning and Cybernetics**: 1–15. DOI: 10.1007/s13042-022-01666-9.

[17] Y. Xu, D. Shen, and X. Bu, (2017) *"Zero-error convergence of iterative learning control using quantized error information"* **IMA Journal of Mathematical Control and Information *34***(3): 1061–1077.

[18] D. Shen and Y. Xu, (2016) *"Iterative learning control for discrete-time stochastic systems with quantized information"* **IEEE/CAA Journal of Automatica Sinica *3***(1): 59–67.

[19] S. Lee and H.-J. Song, (2021) *"Accurate statistical model of radiation patterns in analog beamforming including random error, quantization error, and mutual coupling"* **IEEE Transactions on Antennas and Propagation *69***(7): 3886–3898.

[20] S. Liu, B. Niu, G. Zong, X. Zhao, and N. Xu, (2022) *"Data-driven-based event-triggered optimal control of unknown nonlinear systems with input constraints"* **Nonlinear Dynamics *109***(2): 891–909.

[21] Z. Hou and S. Jin, (2010) *"A novel data-driven control approach for a class of discrete-time nonlinear systems"* **IEEE Transactions on Control Systems Technology *19***(6): 1549–1558.

[22] Y. Zhao, X. Liu, H. Yu, and J. Yu, (2020) *"Model-free adaptive discrete-time integral terminal sliding mode control for PMSM drive system with disturbance observer"* **IET Electric Power Applications *14***(10): 1756–1765.

[23] X. Bu, Y. Qiao, Z. Hou, and J. Yang, (2018) *"Model free adaptive control for a class of nonlinear systems using quantized information"* **Asian Journal of Control *20***(2): 962–968.

[24] H. Zhang, J. Zhou, Q. Sun, J. M. Guerrero, and D. Ma, (2015) *"Data-driven control for interlinked AC/DC microgrids via model-free adaptive control and dual-droop control"* **IEEE Transactions on Smart Grid *8***(2): 557–571.

[25] Y. Weng and X. Gao, (2016) *"Data-driven robust output tracking control for gas collector pressure system of coke ovens"* **IEEE Transactions on Industrial Electronics *64***(5): 4187–4198.

[26] S. Zhang, P. Zhou, Y. Xie, and T. Chai, (2022) *"Improved model-free adaptive predictive control method for direct data-driven control of a wastewater treatment process with high performance"* **Journal of Process Control *110***: 11–23.

[27] D. Xu, Y. Shi, and Z. Ji, (2017) *"Model-free adaptive discrete-time integral sliding-mode-constrained-control for autonomous 4WMV parking systems"* **IEEE Transactions on Industrial Electronics *65***(1): 834–843.

[28] X. Li, C. Ren, S. Ma, and X. Zhu, (2020) *"Compensated model-free adaptive tracking control scheme for autonomous underwater vehicles via extended state observer"* **Ocean Engineering *217***: 107976.

[29] X. Bu, P. Zhu, Q. Yu, Z. Hou, and J. Liang, (2020) *"Model-free adaptive control for a class of nonlinear systems with uniform quantizer"* **International Journal of Robust and Nonlinear Control *30***(16): 6383–6398.

[30] H. Zhao, L. Peng, and H. Yu, (2022) *"Quantized model-free adaptive iterative learning bipartite consensus tracking for unknown nonlinear multi-agent systems"* **Applied Mathematics and Computation *412***: 126582.